Available online at www.sciencedirect.com

SCIENCE DIRECT®

Journal of Molecular Catalysis A: Chemical 199 (2003) 65–71

JOURNAL OF MOLECULAR CATALYSIS A: CHEMICAL

www.elsevier.com/locate/molcata

STM observation of molecular chirality and alignment on solid surface

Masahiro Taniguchi [a,*], Hiroko Nakagawa [b], Akihiko Yamagishi [c], Kohichi Yamada [b]

[a] *Division of Biological Sciences, Graduate School of Sciences, Hokkaido University, N10 W8, Kita-ku, Sapporo 060-0810, Japan*
[b] *Faculty of Pharmaceutical Sciences, Josai University, Sakaido, Saitama 350-02, Japan*
[c] *Department of Earth and Planetary Science, Graduate School of Science, The University of Tokyo, 7-3-1, Hongo, Bunkyo-ku, Tokyo 113-0033, Japan*

Received 20 May 2002; received in revised form 20 November 2002; accepted 20 November 2002

Abstract

Two-dimensional adlayer of a helically shaped aromatic compound, hexathia[11]heterohelicene ([11]TH), which consists of fused five benzene rings and six thiophene rings, was prepared on Au(1 1 1), Au(1 1 0) and polycrystalline gold under UHV condition. LEED and STM were used for characterization of alignment, ordering and chirality of [11]TH on these Au substrates. A [11]TH monolayer on Au(1 1 1) showed the presence of an adlayer lattice with six-fold symmetry, while [11]TH on Au(1 1 0) did align along $\langle 1\,\bar{1}\,0\rangle$ direction, and [11]TH adsorbed on a step bunching area formed chiral sensitive arrays, being one-dimensionally aligned chains. These observations are discussed in terms of stereoselective interaction among [11]TH's, which is strongly affected by the surface structure of a substrate.

Keywords: Scanning tunneling microscopy; Helicene; Chemisorption; Gold surface; Chiral discrimination

1. Introduction

Chirality is usually recognized by chemists in the form of molecular structure, not as a bulk property. Accordingly the mechanistic models for asymmetric syntheses or optical resolution are postulated in terms of stereoselective molecular interaction. So far, however, experimental observation that leads to the elucidation of such mechanisms has been mostly restricted to the properties of a gross material. For example, measurements by circular dichroism (CD) and optical rotatory dispersion (ORD) give the averaged chiral properties of a large number of molecules in a sample. A commonly used index, "enantiomer excess (e.e.)", is merely a balancing factor of two opposite enantiomers.

In contrast to these traditional studies on chemical reactions involving chiral molecules, it is now attempted to reveal the role of molecular chirality by direct observation of an individual molecule. For that purpose, it is most desirable to discriminate each optical isomer. The possibility of realizing such observation is highly dependent on the spatial resolution of observation techniques. Scanning probe microscopy (SPM) provides us with resolution high enough for identification of isomer states. In the previous works, enatiomorphous and racemic domains were structurally discriminated successfully by the application of SPM for two-dimensional systems such

* Corresponding author. Present address: Department of Materials Science and Engineering, Kanazawa Institute of Technology, 7-1 Ohgigaoka, Nonoichi, Ishikawa-gun, Ishikawa 921-8501, Japan. Tel.: +81-76-248-9435; fax: +81-76-294-6704.
E-mail address: taniguchi@neptune.kanazawa-it.ac.jp (M. Taniguchi).

1381-1169/03/$ – see front matter
doi:10.1016/S1381-1169(03)00019-0

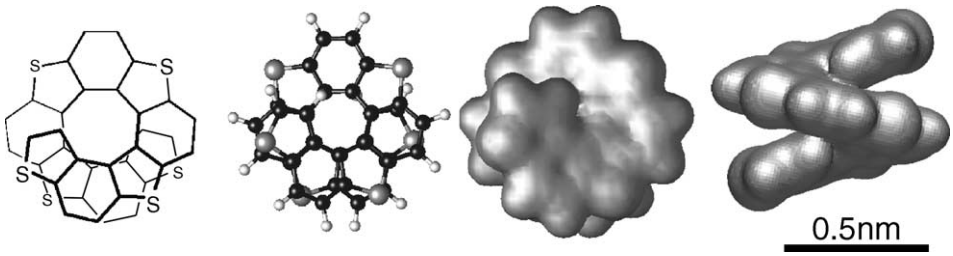

Fig. 1. The structure and models of M-isomer of thia[11]heterohelicene ([11]TH). The structure and the electron distribution were calculated using MOPAC93. The antipode of M-isomer is called P-isomer. Middle-left: calculated structure of M-[11]TH; middle-right: electron distribution viewed along the helical axis; far-right: viewed along the two-fold symmetry axis.

as Langmuir–Blodgett films, self-assembled films, liquid crystals, etc. [1–9]. Chiral patchwork systems (racemic conglomerates) investigated in the previous works are of a promising candidate for homo-chiral two-dimensional systems. They are possible to be used as heterogeneous catalyst of asymmetric reaction or separation media for optical resolution.

SPM images under sufficiently high resolution [10–20] will discriminate not only domain chirality but also molecular chirality, from which the absolute configuration of a discrete molecule can be determined [21–24]. Image resolution is further enhanced by the cooperation of other factors such as the size and shape of a target molecule.

In this study, we have attempted the direct discrimination of molecular chirality on gold surfaces using scanning tunneling microscope (STM) [25,26]. A compound imaged here is hexathia[11]heterohelicene, denoted as [11]TH. [11]TH consists of five benzene rings and six thiophene rings being an angularly annulated aromatic molecule [27–31]. It has such a helical shape as can be compared to a spring washer of double decker. As expected from its structure, [11]TH has a high energy barrier for racemization ($\Delta G^{\ddagger} >$ 200 kJ/mol at 500 K), and the formation of chiral sensitive domain may not be accomplished by racemization but by lateral diffusion/rearrangement on a surface.

The asymmetric structure of helicenes has been studied by spectroscopic methods such as non-linear optical spectroscopy and circular dichroism [32,33]. The series of helicene moiety are introduced in polymers and in macromolecules as a chiral center, asymmetric chromophore, and optical sensitizer. In the imaging of molecular chirality by STM, helical anisotropy in σ-orbital shape of [11]TH of Fig. 1 is expected to be more favored than an asymmetric carbon atom constituted by organic functional groups.

2. Experimental

[11]TH, prepared according to [27–29], was vaporized to form adlayer on an Au substrate in a home-made evaporator directly mounted onto the main UHV chamber as follows. The base pressure of the system was lower than 5×10^{-8} Pa after the baking-out at 135 °C for 24 h. No contamination caused by [11]TH evaporation was found when it was kept at room temperature. Twenty milligrams of racemic-[11]TH powder was stuffed into a Pyrex glass tube of 2 mm ∅ with tungsten heating coil. [11]TH adlayer preparation was controlled by changing the exposure time as the heating power was kept constant. A gold substrate was kept at room temperature during [11]TH adlayer preparation. It took ca. 600 s for adlayer preparation by monolayer in a typical condition ($T_{evap} \cong 430$ K). Pressure during the preparation was kept lower than 2×10^{-7} Pa.

Au(1 1 1) and Au(1 1 0) single crystals (purchased from MaTecK GmbH, Germany) were cleaned by Ar^{+} sputtering and annealing, respectively. These gold surfaces showed reconstructed (1 1 1)-$\sqrt{3} \times 23$ and (1 1 0)-1 × 2 LEED patterns after cleaning. A gold film epitaxially grown on mica in the same UHV system was also used as a substrate. The film was imaged to ensure a reconstructed-(1 1 1) surface with hexagonal facets. Thereafter, [11]TH was evaporated without exposure to an atmosphere. All STM topographic images were acquired in the constant current

mode using JEOL JSTM-4600 scanning tunneling microscope with home-built sample treatment facility. No enhancement except background correction was performed.

3. Results

In the low coverage region ($\theta = 0.05$), [11]TH was found to be adsorbed preferentially on either narrow terraces or steps but not on a wide (1 1 1) terrace. With the increase of coverage, molecules were adsorbed to form a monolayer on a wide terrace. Fig. 2 shows one of the molecular resolution images under such conditions. The molecular spacing was found to be nearly constant at 1.2 nm though the lateral ordering of molecules was not clearly seen. Most interestingly the helicity of an individual molecule can be distinguishable when its image is compared to the molecular model in Fig. 1. As a result, it was concluded that there was no regularity in either in-plane distribution of P- and M-isomers or lateral orientation. Thus the molecules were interacting with little discrimination of chirality at a lower coverage.

With the further increase of coverage, [11]TH was found to form an ordered monolayer on (1 1 1) terraces as shown in Fig. 3. Domain size was found to be larger than 50 nm in a flat region. The [11]TH monolayer showed a hexagonally packed lattice with the molecule–molecule spacing of 1.2 nm. The molecular spacing observed here (1.2 nm) well corresponds to the molecular geometry when projected with its aromatic rings lying flat on the substrate. [11]TH overlayer was found to show similar structure on two substrate or reconstructed Au(1 1 1)-$\sqrt{3} \times 23$ and its analogue of gold film epitaxially grown on mica.

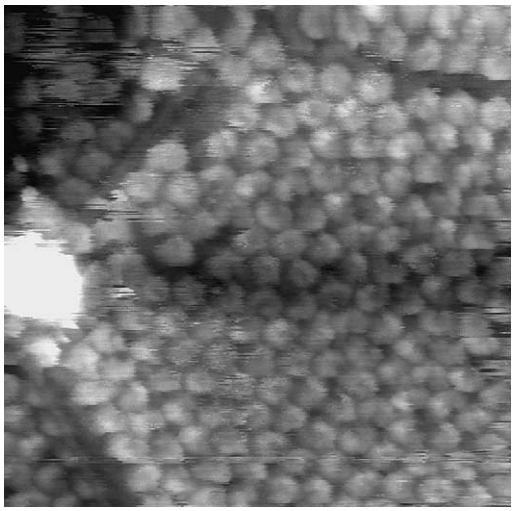

Fig. 2. The [11]TH monolayer imaged on a terrace top region of Au(1 1 1). Scanned area: 20 nm × 20 nm; sample bias +1.6 V; tunneling current 1.0 nA.

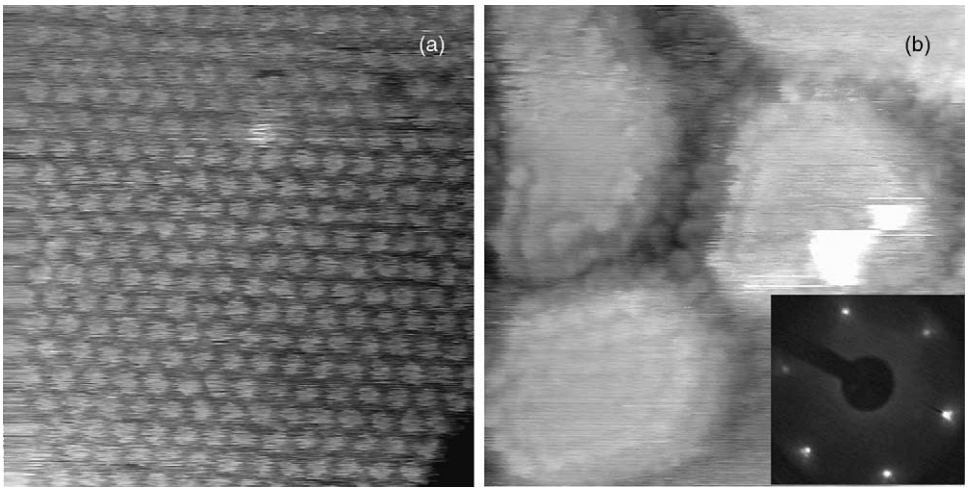

Fig. 3. The [11]TH monolayer imaged on Au(1 1 1). (a) On the wide terrace: 20 nm × 20 nm; bias: +1.2 V; current: 1.8 nA. (b) Monoatomic islands covered by [11]TH. Inset: LEED pattern ($E_p = -59$ eV) showing the orientation of the crystal imaged in (b).

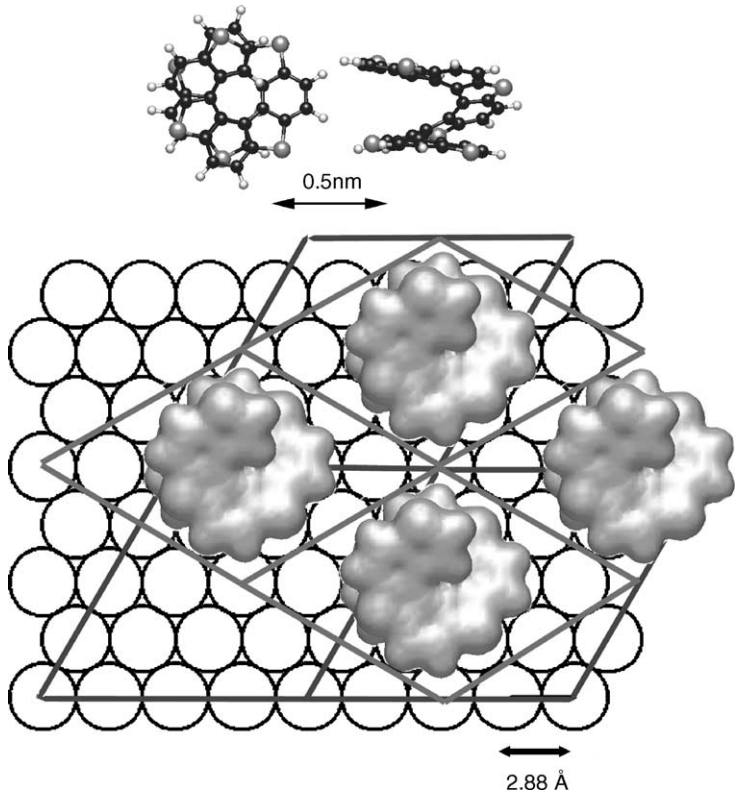

Fig. 4. Size comparison between the hexagonal lattice of Au(1 1 1) and the tentatively proposed [11]TH lattice.

The rotation angle of [11]TH layer was determined to be 30° against hexagonal lattice of Au(1 1 1) in comparing the LEED pattern with STM image in the hexagonal lattice as shown in Fig. 3. The pattern changed from $\sqrt{3} \times 23$ to diffuse 1×1 with the increase of the evaporation amount. This suggests the rebounds of the substrate structure to 1×1 by the adsorption of [11]TH molecules.

Fig. 4 shows a proposed model showing the relative position between the substrate lattice and the [11]TH lattice. At rotation angle 0°, the simple $P(4 \times 4)$ structure (lattice size: 1.15 nm) is suggested for the observed structure. The lattice mismatch is negligible under this condition. Contrary to this, when the rotation angle was 30° as the lattice size 0.996 nm $(2\sqrt{3} \times \sqrt{3})$ R 30°, no consistent model with the image in Fig. 3 was found.

High ordering and symmetry indicated no chirality recognition between P- and M-enantiomers in this hexagonal phase. This is because the formation of ordered racemic phase must have lower symmetry and domain boundaries on the six-fold symmetry substrate. A racemic pair of P- and M-enantiomers is not expected to show the six-fold symmetry but some lower symmetry such as three-fold symmetry including periodic vacant sites or such as two-fold symmetry of fully packed racemic pairs. The fact that the large hexagonal domain with no phase boundary was observed suggested that P- and M-enantiomers were randomly distributed in a glassy phase with no chirality recognition between two enantiomers.

A [11]TH monolayer on Au(1 1 0) substrate shows a lower symmetry and ordering as shown in Fig. 5, which shows the $P(1 \times 4)$ LEED pattern and the corresponding STM image. When [11]TH was evaporated on Au(1 1 0)-1×2 surface, [11]TH/Au(1 1 0) showed 1×4 or 4×1(2) LEED patterns separately. The appearance of the 4×1(2) structure was less frequent in the present experiments. The 1×4 structure appeared to be stable even after annealing the sample at

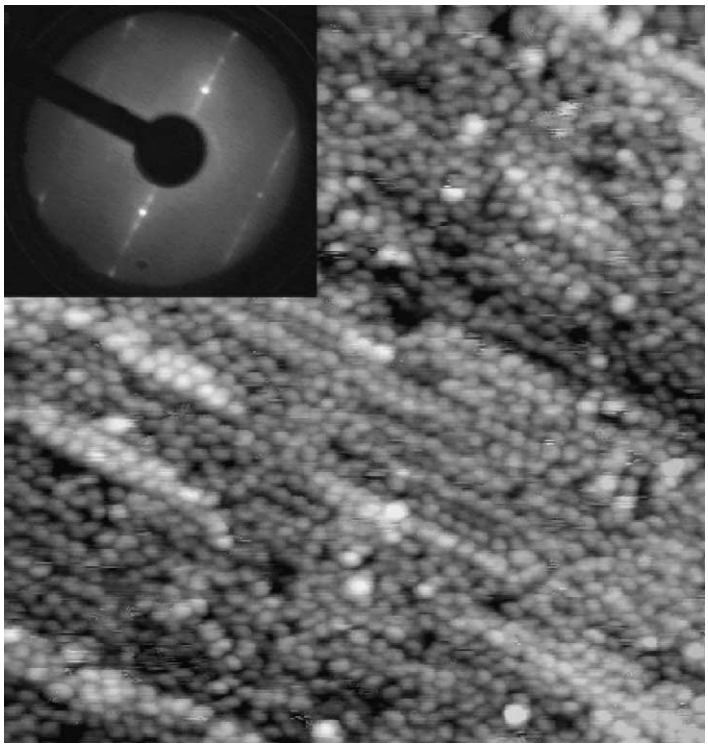

Fig. 5. [11]TH evaporated on Au(1 1 0). Scanned area: 50 nm × 50 nm; sample bias: +2.5 V; tunneling current: 0.5 nA. The inset is the $P(1 \times 4)$ LEED pattern; $E_p = -59$ eV.

360 K. The $P(1 \times 4)$ pattern was observed in the LEED electron energy region E_p higher than 40 eV and no superstructure was observed in the lower energy region. Therefore the $P(1 \times 4)$ LEED pattern should be assigned to the Au(1 1 0) substrate. The STM images of [11]TH/Au(1 1 0) are of one-dimensional alignment to form chains along $\langle 1\,\bar{1}\,0\rangle$ direction but being disordered in $\langle 0\,0\,1\rangle$ direction. The molecular spacings measured in the local domain were 1.1 nm $\langle 1\,\bar{1}\,0\rangle$ and 2.0 nm $\langle 0\,0\,1\rangle$, respectively.

The missing row structure of Au(1 1 0)-1 × 2 has a lattice of 0.288 $\langle 1\,\bar{1}\,0\rangle$ × 0.814 nm $\langle 0\,0\,1\rangle$. In $\langle 0\,0\,1\rangle$ direction, the quadruple periodicity (1.6 nm) obtained from $P(1 \times 4)$ LEED pattern was large enough to accommodate [11]TH molecules. But in $\langle 1\,\bar{1}\,0\rangle$ direction, the lattice size is too small to accommodate them. Though [11]TH chains were clearly imaged on (1 1 0) surface, the chirality of each molecule in a chain was not distinguished yet. The anisotropic property of (1 1 0) substrate was reflected on the ordering of [11]TH but the misfit of lattice

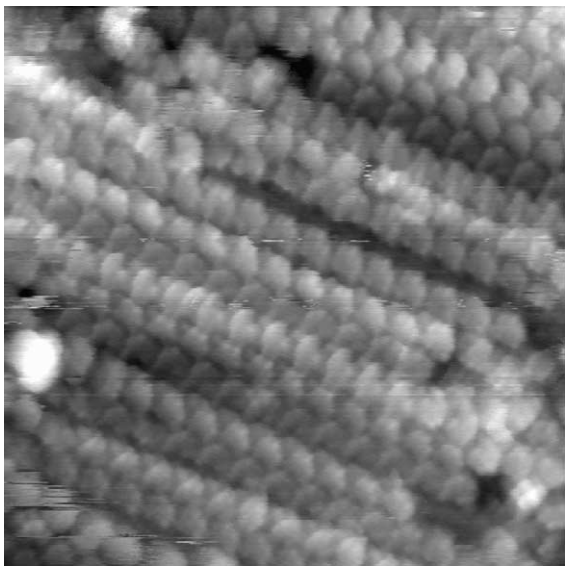

Fig. 6. The [11]TH array imaged in the multi step region of polycrystalline gold film evaporated over mica. Scanned area: 20 nm × 20 nm; bias: −1.6 V; current: 0.91 nA.

size seemed to weaken the selective interaction of chirality.

Fig. 6 shows the image taken in the region consisting of narrow steps on a gold film grown on mica. The film on some higher index surface than (1 1 1) and (1 1 0) did not give an ordered [11]TH chain as observed on (1 1 1) and (1 1 0) substrates. These profiles of [11]TH adlayer suggest that the adsorption geometry on a stepped region is different from that on a flat terrace.

Close examination of Fig. 6 shows that the molecules in each row showed the same handedness. Each row consisted of [11]TH molecules of the same chirality. We emphasize here that the observed twist was not an artifact because different handedness was visible depending on each row in the image of Fig. 6. Moreover the difference between two sequentially acquired images showed a flat featureless image, reflecting that the twist information was sustained in spite of lateral drift. To our knowledge, this is the first direct observation of chiral discrimination in one-dimensional array.

4. Discussion

The behavior of [11]TH adlayer showed a clear dependence on the structure of gold substrate as shown in the cases of (1 1 1), (1 1 0), and epitaxial film on mica. In a racemic crystal, P- (or M-) [11]TH molecules form homo-chiral columns as shown in Fig. 7(a) [34,35]. The P/M-columns are ordered alternatively in the (−1 0 1) plane. Contrary to this pseudo-square lattice, no hexagonal-like packing as observed on (1 1 1) surface was found in the bulk crystal viewed in different cross sections (Fig. 7(b)).

On a gold surface, [11]TH molecules are ordered in a chirality sensitive manner on a step bunching area but not on a flat (1 1 1) area. In the former case, the structure consisted of homo-chiral chain of [11]TH molecules as found in the bulk crystal structure. In the latter case, the molecules are hexagonally packed with no appearance of chiral interaction.

Even in the anisotropic case such as the (1 1 0) surface, no chiral sensitive interaction was not dominant when molecular interaction was operative only in one direction.

It is noteworthy that the molecular array located in ledge site arrays showed some registry mismatch with that of terrace area of the same step plane as shown in Fig. 8. The structure around a step edge suggests the possibility of an ordered lattice with chiral discrimination on an appropriate substrate. The dominant geometry of step edges neighboring to (1 1 1) terrace is similar to that of (1 0 0) or (1 1 0) surface. The higher index surface which consists of steps and narrow ter-

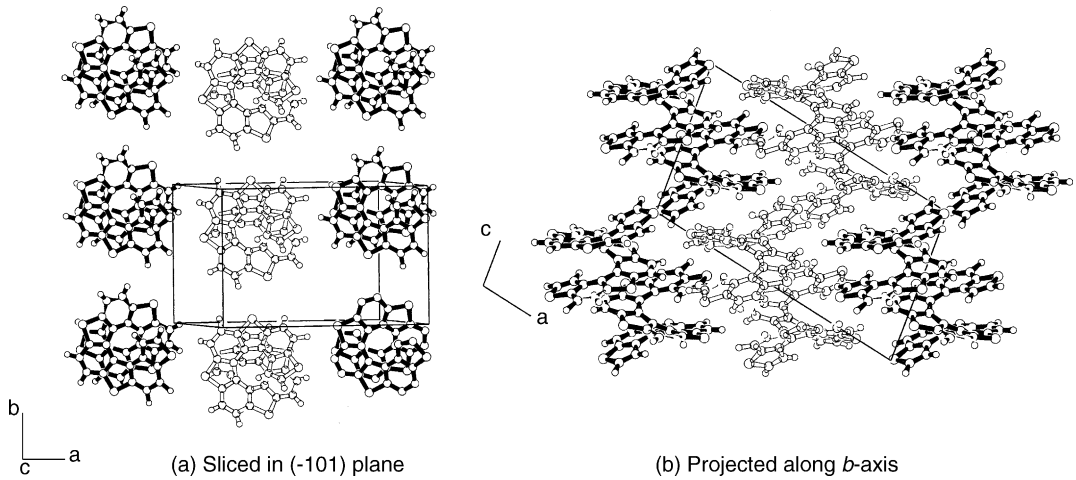

Fig. 7. P-, M-isomers in the bulk crystal of *rac*-[11]TH drawn by ORTEP-III. (a) Sliced in (−1 0 1) plane. (b) Projected along *b*-axis. The lattice parameters used for these drawings are as follows: $a = 20.109$ Å, $b = 11.388$ Å, $c = 11.472$ Å; $\alpha = 92.077°$, $\beta = 101.386°$, $\gamma = 89.568°$. $Z = 4$, space group: $P\bar{1}$.

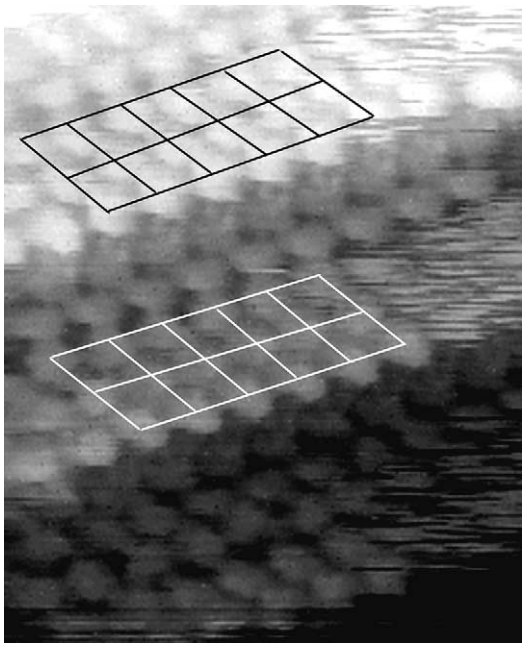

Fig. 8. Mismatch of the ledge site array and the terrace lattice. The [11]TH array at ledge site has mismatch with the regular lattice on the same terrace. Scanned area: 12 nm × 15 nm; bias +1.1 V; current: 0.72 nA. Substrate: polycrystalline gold film evaporated over mica.

races with smaller misfit might reproduce molecular chains with homo-chirality as found on a polycrystalline surface.

References

[1] R. Viswanathan, J.A. Zasadzinski, D.K. Schwarz, Nature 368 (1994) 440.
[2] D.P.E. Smith, J. Vac. Sci. Technol. B 66 (1991) 2096.
[3] S.J. Sowerby, W.M. Heckl, G.B. Peterson, J. Mol. E 43 (1996) 419.
[4] J.P. Rabe, S. Buchholz, Phys. Rev. Lett. 66 (1991) 2096.
[5] C.J. Eckhardt, N.M. Peachy, D.R. Swanson, J.M. Takacs, M.A. Khan, X. Gong, J.-H. Kim, J. Wang, R.A. Uphaus, Nature 362 (1993) 614.
[6] F. Stevens, D.J. Dyer, D.M. Walba, Angew. Chem. 108 (1996) 955.
[7] S.D. Feyter, P.C. Grim, M. Rucker, P. Vanoppen, C. Meiners, M. Sie.ert, S. Valiyaneettil, K. Mullen, F.C.D. Schryver, Angew. Chem. Int. Ed. 37 (1998) 1223.
[8] H. Fang, L.C. Giancarlo, G. Flynn, J. Phys. Chem. 102 (1998) 7311.
[9] D.G. Yablon, C. Giancarlo, G.W. Flynn, J. Phys. Chem. 104 (2000) 7627.
[10] X. Lu, K.W. Hipps, X.D. Wang, U. Mazur, J. Am. Chem. Soc. 118 (1996) 7197.
[11] P.H. Lippel, R.J. Wilson, M.D. Miller, C. Woll, S. Chiang, Phys. Rev. Lett. 62 (1989) 171.
[12] J.-Y. Grand, T. Kunstmann, D.Ho. mann, A. Haas, D. Dietsche, J. Seifritz, R. Moller, Surf. Sci. 366 (1996) 403.
[13] K. Glöckler, C. Seidel, A. Soukopp, M. Sokolowski, E. Umbach, M. Böhringer, R. Bernt, W.-D. Schneider, Surf. Sci. 405 (1998) 1.
[14] U. Stahl, D. Gador, A. Soukopp, R. Fink, E. Umbach, Surf. Sci. 414 (1998) 423.
[15] R. Stromaier, J. Petersen, B. Gompf, W. Eisenmenger, Surf. Sci. 418 (1998) 91.
[16] K. Itaya, Prog. Surf. Sci. 58 (1998) 121.
[17] G.P. Lopinski, D.J. Mo.att, D.D.M. Wayner, M.Z. Zgierski, R.A. Wolkow, J. Am. Chem. Soc. 121 (1999) 4532.
[18] M. Böhringer, K. Morgenstern, W.D. Schneider, R. Berndt, F. Mauri, A.De. Vita, R. Car, Phys. Rev. Lett. 83 (1999) 324.
[19] M. Böhringer, K. Morgenstern, W.D. Schneider, R. Berndt, J. Phys.: Condens. Matter 11 (1999) 9871.
[20] B. Ohtani, A. Shintani, K. Uosaki, J. Am. Chem. Soc. 121 (1999) 6515.
[21] M. Ortega Lorenzo, S. Haq, T. Bertrams, P. Murray, R. Raval, C.J. Baddeley, J. Phys. Chem. B 103 (1999) 10661.
[22] M. Ortega Lorenzo, C.J. Baddeley, R. Raval, Nature 404 (2000) 376.
[23] M. Schunack, E. Lagsgaard, I. Stensgaard, I. Johannsen, F. Besenbacher, Angew. Chem. Int. Ed. 40 (2001) 2623.
[24] A. Kühnle, T.R. Linderoth, B. Hammer, F. Besenbacher, Nature 415 (2002) 891.
[25] M. Taniguchi, H. Nakagawa, A. Yamagishi, K. Yamada, Surf. Sci. 454–456 (2000) 1005.
[26] M. Taniguchi, H. Nakagawa, A. Yamagishi, K. Yamada, Surf. Sci. 507–510 (2002) 458.
[27] H. Nakagawa, A. Obata, K. Yamada, H. Kawazura, M. Konno, H. Miyamae, J. Chem. Soc. Perkin Trans. 2 (1985) 1899.
[28] H. Nakagawa, H. Nagashima, K. Yamada, H. Kawazura, Acta Cryst. C41 (1985) 778.
[29] K. Yamada, E. Oguma, H. Nakagawa, H. Kawazura, H. Miyamae, Acta Chem. Scand. 50 (1996) 438.
[30] H. Nakagawa, K. Yamada, H. Kawazura, J. Chem. Soc., Chem. Commun. 1989 (1989) 1378.
[31] K. Yamada, H. Nakagawa, H. Kawazura, Bull. Chem. Soc. Jpn. 59 (1986) 2429.
[32] T. Fukumi, S. Sakaguchi, M. Miya, H. Nakagawa, K. Yamada, H. Kawazura, Rev. Laser Eng. 22 (1994) 409.
[33] S. Siocke, S.V. Elshocht, T. Verbiest, A. Persoons, M. Kauranen, K.E.S. Phillips, T.J. Katz, J. Chem. Phys. 113 (2000) 7578.
[34] H. Nakagawa, J. Yoshino, K. Yamada, submitted for publication.
[35] M.N. Burnett, C.K. Johnson, ORTEP-III: Oak Ridge Thermal Ellipsoid Plot Program for Crystal Structure Illustrations, Oak Ridge National Laboratory Report ORNL-6895, 1996.